Structure of the chlorobenzene–argon dimer: Microwave spectrum and *ab initio* analysis

Jung Jin Oh[a] and Inhee Park
Department of Chemistry, SookMyung Women's University, Seoul, Korea

Robb J. Wilson
Department of Chemistry and Physics, Louisiana State University at Shreveport, Shreveport, Louisiana 71115

Sean A. Peebles and Robert L. Kuczkowski[a]
Department of Chemistry, University of Michigan, Ann Arbor, Michigan 48109-1055

Elfi Kraka and Dieter Cremer[a]
Department of Theoretical Chemistry, Göteborg University, S-41320 Göteborg, Reutersgatan 2, Sweden

(Received 14 July 2000; accepted 1 September 2000)

The rotational spectra of the ^{35}Cl and ^{37}Cl isotopes of the chlorobenzene–argon van der Waals dimer have been assigned using Fourier transform microwave spectroscopy techniques. Rotational constants and chlorine nuclear quadrupole coupling constants were determined which confirm that the complex has C_s symmetry. The argon is over the aromatic ring, shifted from a position above the geometrical ring center towards the substituted carbon atom, and at a distance of about 3.68 Å from it. This distance is 0.1–0.2 Å shorter than the similar distance in the benzene–argon and fluorobenzene–argon complexes. Experimental results are confirmed and explained with the help of second-order Møller–Plesset perturbation calculations using a VDZP+diff basis set. The complex binding energy of the chlorobenzene–argon complex is 1.28 kcal/mol (fluorobenzene–argon, 1.17; benzene–argon, 1.12 kcal/mol) reflecting an increase in stability caused by larger dispersion interactions when replacing one benzene H atom by F or by Cl. The structure and stability of Ar·C_6H_5–X complexes are explained in terms of a balance between stabilizing dispersion and destabilizing exchange repulsion interactions between the monomers. © *2000 American Institute of Physics.* [S0021-9606(00)01644-5]

I. INTRODUCTION

The dimers between rare gases (RG) and aromatic molecules have been of considerable interest to theoretical and experimental structure chemists for approximately 25 years. Over the last decade, the application of high resolution microwave spectroscopy[1] and *ab initio* techniques[2] have been brought to bear intensively on a variety of systems. A prototype investigation was the precise determination of the structure of the benzene–Ar dimer.[3] Our laboratory has recently investigated the fluorobenzene complexes with Ne and Ar.[4,5] These studies showed that the rare gas atom moves slightly closer to the ring and shifts from the ring center towards the fluorinated carbon atom. The distance to the ring is further shortened as more fluorines are added to the ring.[6–10] It was suggested that these structural changes might be associated with the reduced repulsive interactions due to fluorination at the substituted carbon in analogy to arguments used by Kraka *et al.* in studies of heterocyclic–RG compounds.[11,12]

It seemed worthwhile to compare the fluorobenzene results to a chlorobenzene–rare gas complex, since chlorine is larger and more polarizable albeit less electronegative. This paper will report on the structure of the chlorobenzene–argon complex deduced from its rotational spectrum. The Ar atom is again found above the ring shifted towards the substituted carbon atom. It has moved slightly closer to this carbon atom and to the ring compared to fluorobenzene in line with a previous low resolution study and modeling calculations of the chlorobenzene–argon dimer.[13,14] *Ab initio* calculations carried out in the present work verify the experimental structure and provide a basis to rationalize the structure and stability of the chlorobenzene–argon dimer and related complexes.

II. EXPERIMENT

The chlorobenzene–Ar complex was generated by supersonic expansion of about 1–2 bars of argon in the presence of the vapor above some liquid chlorobenzene at room temperature. The transitions were more intense when the argon was bubbled through a sample of liquid chlorobenzene before reaching the nozzle. The chlorobenzene was used without purification from samples obtained from Fisher Scientific.

The rotational transitions were observed with a Balle–Flygare-type Fourier-transform microwave spectrometer[15] which operated between about 6–17 GHz. The spectrometer was recently upgraded for automatic scanning using software and hardware modifications developed at the University of Kiel.[16] Peak frequencies were reproducible to about 4 kHz. The pulsed nozzle was a General Valve Series 9 model with a 0.8 mm diameter orifice. It was controlled by a General Valve Iota One pulse controller at a repetition rate of about 10 Hz. The gas expansion was directed perpendicular

[a]Authors to whom correspondence should be addressed.

TABLE I. Observed rotational transition frequencies (MHz) for Ar–C_6H_5Cl.

			Ar–$C_6H_5{}^{35}Cl$		Ar–$C_6H_5{}^{37}Cl$					Ar–$C_6H_5{}^{35}Cl$		Ar–$C_6H_5{}^{37}Cl$	
$J'K_p'K_o'\leftarrow J''K_p''K_o''$	$2F'$	$2F''$	ν/MHz	$\Delta\nu^a$	ν/MHz	$\Delta\nu^a$	$J'K_p'K_o'\leftarrow J''K_p''K_o''$	$2F'$	$2F''$	ν/MHz	$\Delta\nu^a$	ν/MHz	$\Delta\nu^a$
a-type								11	9	9078.196	5	8925.639	6
4 1 4←3 1 3	11	9	6171.644	1			5 2 3←4 2 2	7	5	9308.247	5		
	5	3	6170.841	9				13	11	9307.247	−3		
	9	7	6170.325	1				9	7	9307.019	−4		
	7	5	6169.512	−2				11	9	9306.030	1		
4 0 4←3 0 3	11	9	6219.819	1			6 1 5←5 1 4	9	7	9995.589	3	9838.371	−6
	5	3	6219.565	3				15	13	9994.936	−2	9837.912	3
	9	7	6217.434	4				11	9	9992.585	−1	9836.117	−4
	7	5	6217.161	−3				13	11	9991.938	−1	9835.660	7
4 2 3←3 2 2	11	9	6811.338	−2			6 2 4←5 2 3	9	7	10954.431	4		
	7	7	6810.354	−14[b]				15	13	10953.411	0		
	7	5	6810.383	4				11	9	10951.723	−1		
	9	7	6809.861	−1				13	11	10950.706	−3		
4 1 3←3 1 2	11	9	7138.372	−3			*b*-type						
	7	5	7136.656	−4			4 0 4←3 1 3	11	9	6149.531	−1	6043.034	4
	9	7	7134.590	7				9	7	6148.626	0	6042.302	5
5 1 5←4 1 4	13	11	7628.516	2	7499.699	1		5	3	6148.574	−1		
	7	5	7627.966	−5	7499.253	−4		7	5	6147.667	−5		
	11	9	7627.439	−5	7498.870	−1	4 1 4←3 0 3	11	9	6241.930	1	6141.507	1
	9	7	7626.903	0	7498.433	0		5	3	6241.821	1	6141.362	6
5 0 5←4 0 4	13	11	7644.386	5	7516.762	−2		9	7	6239.130	3	6139.399	−2
	7	5	7643.952	−4	7516.407	−3		7	5	6239.003	−3	6139.242	−3
	11	9	7642.999	−2	7515.708	0	5 0 5←4 1 4	13	11	7622.271	0	7492.747	0
	9	7	7642.575	0	7515.355	0		7	5	7621.695	−3	7492.283	−1
5 2 4←4 2 3	7	5	8377.412	−1				11	9	7621.307	4	7491.999	−1
	13	11	8377.012	−5				9	7	7620.734	0	7491.535	−4
	9	7	8375.647	3			5 1 5←4 0 4	13	11	7650.625	1	7523.716	2
	11	9	8375.249	4				7	5	7650.224	−5	7523.383	−1
5 1 4←4 1 3	7	5	8603.861	0	8469.276	−1		11	9	7649.141	0	7522.578	−2
	13	11	8602.549	−3	8468.349	0		9	7	7648.743	−2	7522.250	1
	9	7	8599.867	−1	8466.353	5	6 0 6←5 1 5	15	13	9073.246	5	8919.692	−1
	11	9	8598.564	2	8465.418	−3		9	7	9072.819	2	8919.345	−6
6 1 6←5 1 5	15	13	9074.892	−2	8921.562	−17[b]		13	11	9072.441	−2	8919.072	−8
	9	7	9074.482	6	8921.243	2		11	9	9072.025	3	8918.737	−3
	13	11	9074.066	−6			6 1 6←5 0 5	15	13	9081.136	0	8928.531	2
	11	9	9073.657	1				9	7	9080.744	−5	8928.216	1
6 0 6←5 0 5	15	13	9079.485	1	8926.644	1		13	11	9080.209	−4	8927.826	8
	9	7	9079.088	−2	8926.326	2		11	9	9079.826	0	8927.507	3
	13	11	9078.598	15[b]	8925.975	24[b]							

[a]$\Delta\nu=\nu_{obs}-\nu_{calc}$ in kHz.
[b]Not included in the fit. The transitions are not fully resolved due to other components nearby and Doppler effects.

to the mw cavity axis, resulting in linewidths of ~30 kHz FWHM with Doppler splitting usually unresolved.

III. SPECTRAL ANALYSIS AND RESULTS

A. Spectra

A model for the complex based on the fluorobenzene–Ar structure with C_s symmetry (*ab* symmetry plane) was used to predict regions to expect transitions. The model predicted *a*- and *b*-type transitions of about equal intensity and candidates were readily found near the expected regions. The transitions were split into multiplets due to coupling of the chlorine nuclear electric quadrupole moment with the rotational motion (^{35}Cl, $I=3/2$, 75.5% abundance; ^{37}Cl, $I=3/2$, 24.5%). Several regions were characterized by close pairs of *a*- and *b*-*R* branch multiplets which, aided by trial and error using model predictions, led to the correct initial assignment. The four strongest components of each $J\rightarrow J+1$ multiplet were usually measured. They were fit using the SPFIT global-fit program employing 3 rotational constant and 5 centrifugal distortion constants.[17] The coupling scheme used was $I+J=F$, and coupling constants χ_{aa} and $(\chi_{bb}-\chi_{cc})$ were fit. After the more abundant ^{35}Cl isotopomer was assigned, the ^{37}Cl species was measured and assigned in a similar fashion. Table I lists the transition frequencies, most of which were fit to about 5 kHz with a Watson *A*-reduction Hamiltonian, I^r representation.[18] For the weaker ^{37}Cl species, several distortion constants were fixed to the values of the ^{35}Cl isotopomer. The spectral constants from the fit are given in Table II.

B. Structure

The initial stacked structure with the argon above the ring provided a good model to estimate the spectral patterns. After assignment of the transitions, there was no doubt that the complex had this configuration and possessed an *ab* inertial symmetry plane based on the selection rules, quadru-

pole coupling constants and inertial moments. Comparisons of the pertinent planar inertial moments (P_{xx}) and chlorine quadrupole coupling constants (χ_{xx}) to chlorobenzene, which lies in an *ab* symmetry plane with the *b* axis perpendicular to the C_2 axis, are given in Table III. The small differences between P_{cc}(complex) and P_{bb}(monomer), χ_{cc}(complex), and χ_{bb}(monomer) are typical for weakly bound rare gas complexes. They arise mostly from large amplitude vibrational effects on the vibrationally averaged ground state parameters, rather than from structural or electronic reorganization in the complex.

One can determine from the Ar–$C_6H_5{}^{35}Cl$ moments of inertia that the argon is about 3.57 Å (R_{cm}) from the center-of-mass of the chlorobenzene and that the angle between R_{cm} and the C_2 axis of the chlorobenzene is about 80.3°. However, two different structures will fit this model depending on the direction of the angle. These two structures are illustrated in Fig. 1. The structures differ depending on whether the argon shifts about 0.6 Å from a point directly above the c.o.m. of the chlorobenzene either away from the chlorine atom (structure I) or towards it (structure II). The chlorine atom coordinates are considerably different in the two forms, and hence the isotope shift for the Ar–$C_6H_5{}^{37}Cl$ species can readily distinguish between the two possibilities. This is illustrated in Table IV where the predicted rotational constants for the ^{37}Cl species for the two structures are compared with experiment. Only structure I is consistent with the data.

The preferred structural parameters are obtained by using a model first proposed by Klots *et al.*[19] and extended by Bauder in studies of furan–RG (Ref. 7) and pyridine–RG (Ref. 20) complexes. It partially accounts for the large amplitude vibrational wagging motions in these complexes with a planar aromatic partner. The model assumes that the parameters of chlorobenzene are unchanged by complex formation. The vibrational motion is described as a precession about the *c* axis of the monomer which is averaged with a value of $\langle\alpha\rangle$ for this angular deformation. The center-of-mass distance (R_{cm}) between the rare gas and the ring, the angle (θ) formed between R_{cm} and the perpendicular to the ring, and $\langle\alpha\rangle$ are obtained by fitting the three ground state moments of inertia for an isotopomer (see Fig. 2). This model is described more fully in the literature.[5,7,20]

The values determined for R_{cm}, θ, and $\langle\alpha\rangle$ are given in Table V. These are considered the so-called effective or r_0 parameters in the ground vibrational state. Experimental uncertainties based on the rotational constants are about 0.0001 Å, 0.001° and 0.05°, respectively. Model errors are more difficult to estimate; we suggest that these values may differ by 2%–4% from the true equilibrium values.[5] R_{cm} and θ can be used to calculate alternative parameters, the perpendicular distance of the argon to the ring ($R_\perp$), and its shift parallel to the ring plane from the center-of-mass of the chlorobenzene

TABLE II. Spectroscopic constants for argon–chlorobenzene.

	Ar–$C_6H_5{}^{35}Cl$	Ar–$C_6H_5{}^{37}Cl$
A/MHz	1356.1614(23)	1344.5050(35)
B/MHz	1005.4701(8)	987.7036(12)
C/MHz	720.9445(31)	708.5047(34)
Δ_J/kHz	4.810(13)	4.803(6)
Δ_{JK}/kHz	−18.208(91)	−18.724(84)
Δ_K/kHz	25.83(44)	25.83[c]
δ_J/kHz	2.0753(88)	2.0753[c]
δ_K/kHz	0.290(108)	0.290[c]
χ_{aa}	−2.935(28)	−5.596(58)
χ_{bb}	−35.419(21)	−24.631(33)
$\Delta\nu_{rms}$/kHz[a]	3.20	3.50
N[b]	75	44

[a]$\Delta\nu = \nu_{obs} - \nu_{calc}$.
[b]Number of transitions in the fit.
[c]Distortion constants were fixed to the value for the main isotopic species.

TABLE III. Inertial planar moments and chlorine quadrupole coupling constants for the chlorobenzene–argon and chlorobenzene monomer.

	Ar–$C_6H_5{}^{35}Cl$[c]	$C_6H_5{}^{35}Cl$[d]	Ar–$C_6H_5{}^{37}Cl$	$C_6H_5{}^{37}Cl$
P_{aa}[a]	415.4856	320.5345	424.5473	329.7352
P_{bb}	285.5086	89.1187	288.7561	89.1190
P_{cc}	87.1460	0.0453	87.1284	0.0464
χ_{aa}[b]	−2.94	−71.25	−5.60	−56.10
χ_{bb}	−35.42	36.88	−24.63	29.03
χ_{cc}	38.36	34.37	30.23	27.07

[a]$2P_{xx} = I_y + I_z - I_x = 2\Sigma m_i x_i^2$ (in $u\cdot$Å^2). $I_x \cdot B_x = 505\,379.0$ MHz$\cdot u\cdot$Å^2.
[b]$\chi_{xx} = eQq_{xx}$ (in MHz); $\chi_{aa} + \chi_{bb} + \chi_{cc} = 0$.
[c]Data for chlorobenzene–Ar from this work.
[d]Data for chlorobenzene monomer from Ref. 21 except χ_{aa} for the ^{37}Cl species from Ref. 22 and assuming $\eta = -0.035$.

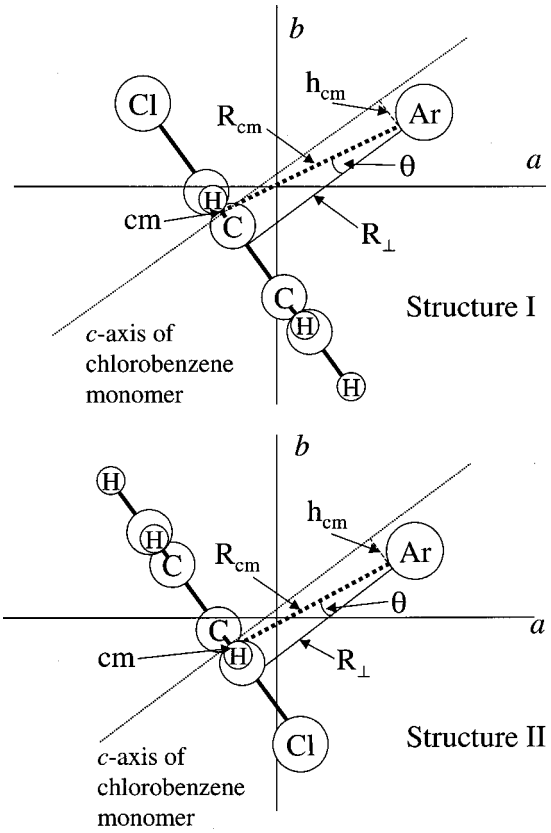

FIG. 1. Two possible structures of chlorobenzene–argon consistent with the data from one isotopic species. Only structure I is consistent with data from the ^{35}Cl and ^{37}Cl isotopomers.

TABLE IV. Comparison of the observed rotational constants (MHz) of Ar–$C_6H_5{}^{37}Cl$ with predicted values for two possible structures.

Rotational constant	Structure I	Structure II	Experiment
A	1339.7	1318.7	1344.5
B	985.0	1002.0	987.7
C	709.8	712.5	708.5

(h_{CM}). While h_{CM} is useful to describe the structure of the complex on the basis of the spectroscopic analysis, the parameter $R_{\|}$ (indirectly related to h_{CM}) is more useful for the electronic analysis of the argon complex. It defines the horizontal shift of the Ar atom away from a position above the geometrical center of the benzene ring towards ($R_{\|}>0$) or away from ($R_{\|}<0$) the substituted C atom (see Fig. 2). Parameter $R_{\|}$ is zero for the benzene–argon complex and becomes larger than zero for halobenzene–argon complexes. For the chlorobenzene–argon complex, the argon is shifted ($R_{\|}$) about 0.38 Å from the center of the ring (see below).

IV. QUANTUM CHEMICAL INVESTIGATION

The requirements for getting a reliable description of argon van der Waals complexes are well-known (see, e.g., discussion in Ref. 11): (1) large basis sets, which correctly reproduce the polarizabilities of the complex partners must be used; (2) basis set consistent calculations, i.e., all calculations including geometry optimizations and property calculations have to be corrected for basis set superposition errors (BSSEs); (3) a size extensive correlation corrected *ab initio* method has to be applied.

In the case of the benzene–argon complex, Koch and co-workers[2] obtained a reliable complex binding energy ΔE(complex) at the CCSD(T)/aug-cc-pVQZ level of theory where the effect of the aug-cc-pVQZ basis was estimated with the help of MP2/aug-cc-pVQZ calculations. Smaller basis sets of the aug-cc-pVmZ type ($m=2$ or 3) or a lower level of theory (CCSD, MP2) implied errors up to 35% in the ΔE(complex) of benzene–argon.[2] However, due to a fortuitous cancellation of basis set and correlation errors the MP2/aug-cc-pVDZ result turned out to reproduce the experimental complexation energy rather accurately.

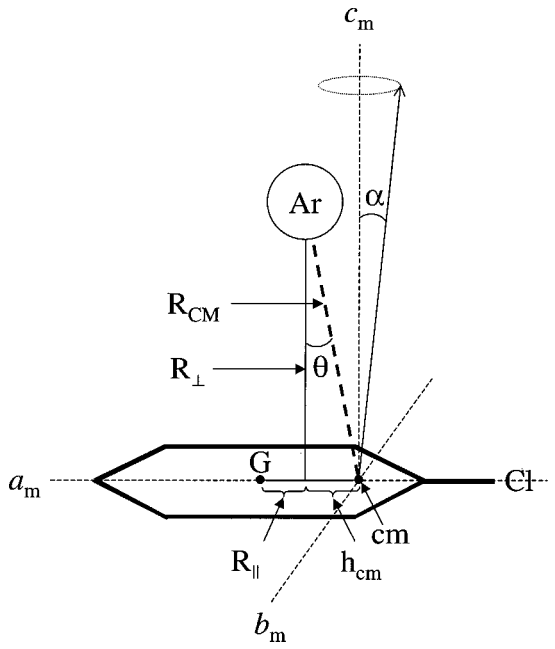

FIG. 2. Definition of the structural parameters used in Tables V and VI. R_{cm}, θ, and $\langle\alpha\rangle$ are determined from Bauder's equations (Ref. 20). a_m, b_m, c_m indicate the position of the principal axes of chlorobenzene monomer from its center-of-mass at point cm. Point G is the geometric center of the monomer ring. $R_{\|}$ and h_{cm} are distances between these ring points and the intersection of $R_\perp$ and the ring plane.

In this work, we are predominantly interested in the changes in the properties of Ar·C_6H_5–X complexes upon replacing X and, therefore, we have sacrificed computational accuracy [e.g., achieved by applying coupled cluster (CC) methods such as CCSD(T) with a large basis set] by employing just second order Møller–Plesset (MP2) perturbation theory[23] with an augmented VDZ basis set to reduce computational cost. MP2 covers electron pair correlation effects and, by this, is able to give a reasonable description of dispersion interactions between the monomers of a van der Waals complex, which may lead to rather accurate ΔE(complex) values as shown for benzene–argon[2] or similar complexes.[11,12]

For the Ar atom, we have chosen the $(14s10p2d1f)\times[7s4p2d1f]$ basis of Chałasinski, Funk, Simons, and Breckenridge[24] since this basis is known to reproduce the Ar polarizability at the MP2 level with an accuracy of 96%. It is

TABLE V. Comparison of structural parameters[a] of aromatic–Ar complexes.

Complex	$R_\perp$	$R_{\|}$	h_{CM}	R_{cm}	θ	$\langle\alpha\rangle$	Ref.
$C_6H_5{}^{35}Cl$–Ar	3.540	0.387	0.563	3.585	9.04	12.2	this work
$C_6H_5{}^{37}Cl$–Ar	3.539	0.379	0.609	3.591	9.76	12.3	this work
C_6H_6–Ar	3.586	0.00	0.00	3.586	0.00	4.81	3
C_6H_5F–Ar	3.572	0.208	0.297	3.584	4.8	9.92	4, 5
1,4-$C_6H_4F_2$–Ar	3.550	0.00	0.00	3.550	0.00	0.00	6
1,2-$C_6H_4F_2$–Ar	3.545	···	0.523[b]	3.583	8.40	7.38	7
1,2,3-$C_6H_3F_3$–Ar	3.522	0.187	0.532	3.562	8.60	4.63	8, 9
1,2,4-$C_6H_3F_3$–Ar	3.517	···	0.379[b]	3.537	6.19	···	10

[a]Distances in Å; angles in deg. R_{cm}, θ, and $\langle\alpha\rangle$ in Fig. 2 are calculated using the equations in Ref. 20 except for C_6H_6–Ar, 1,4-$C_6H_4F_2$–Ar, 1,2,4-$C_6H_3F_3$–Ar. Also see Fig. 2 for explanation of $R_\perp$, $R_{\|}$, and h_{CM}.
[b]There are insufficient data to unambiguously determine the direction of h_{CM} and $R_{\|}$.

TABLE VI. MP2 energies and response properties of chlorobenzene, fluorobenzene, and their corresponding argon complexes.[a]

	Chlorobenzene	Fluorobenzene
$\Delta E(1)$ (kcal/mol)	7.00	7.86
$\Delta E(2)$	1.12	0
μ (Debye)	1.649 (1.69)[b]	1.593 (1.60)[c]
Q_{aa}, Q_{bb}, Q_{cc} (Buckingham)	−48.13, −44.57, −52.68	−42.51, −36.29, −44.30
α_{iso} (Å^3)	12.00 (12.3)[d]	9.91 (10.3)[d]
α_{aa}, α_{bb}, α_{cc}	15.88, 12.77, 7.35	11.88, 11.70, 6.18
Ar-complex		
ΔE(complex) (kcal/mol) {cm^{-1}}	−1.28 {−449}	−1.17 {−409}
μ_{total} (Debye)	1.641	1.599 (1.528)[c]
μ_a, μ_c	1.641, 0.051	1.598, 0.052
Q_{aa}, Q_{bb}, Q_{cc} (Buckingham)	−59.91, −56.36, −65.12	−54.30, −48.08, −56.75
$R_\perp$ (Å)	3.560 (3.540)	3.588 (3.572)
$R_\parallel$	0.233 (0.387)	0.154 (0.228)
$R_{\text{Ar,Cl}}$	3.741 (3.681)	3.790 (3.752)
$R_{\text{Ar,X}}$	4.577 (4.470)	4.411 (4.362)

[a]Reaction energies $\Delta E(1)$ and $\Delta E(2)$ calculated at MP2/G3MP2large refer to isodesmic reactions (1) and (2) as described in the text. Response properties are calculated at MP2/[7s4p2d1f/4s3p1d/3s1p]. Dipole moment, quadrupole moment, and dipole polarizability are denoted by symbols μ, Q, and α, respectively, and components are given in the monomer inertial system. For the definition of their components and for the explanation of $R_\perp$, $R_\parallel$, $R_{\text{Ar,Cl}}$, and $R_{\text{Ar,X}}$, see Fig. 2. Experimental values are given in parentheses where available.

[b]Experimental value from Ref. 32(a).

[c]Experimental values from Ref. 4.

[d]Experimental values from Ref. 39. The calculated value for benzene (optimization of geometry at MP2/G3MP2large and calculation of α with a Spackman basis): $\alpha_{aa}=\alpha_{bb}=11.81$, $\alpha_{cc}=6.33$, $\alpha_{\text{total}}=9.98\,(10.0)^d$ Å^3.

just of DZ+(2d1f) quality (36 basis functions for Ar), but the two most diffuse *sp* functions of the (14s10p) basis are not contracted and the exponents of added *d*- and *f*-type polarization functions are optimized to accurately describe the dispersion energy of Ar_2.

In previous work, Kraka and co-workers[11,12] found that a 6-31G(+sd,+sp) basis derived by Spackman[25] by adding to Pople's 6-31G basis[26] diffuse polarization functions as well as a diffuse *s*-function leads to reasonable polarizabilities of aromatic molecules, which is a prerequisite for reasonably describing van der Waals complexes involving benzene or its derivatives. Spackman optimized the exponents of the *d*-type polarization functions for first- and second-row atoms as well as of the *p*-type polarization functions for hydrogen in the way that the mean polarizability of first- and second-row AH_n hydrides is maximized.[25] The exponent of the diffuse *s* function was set equal to 1/4 of the value of the outermost *sp* functions of the original 6-31G basis, while the exponent of the diffuse *s* function for hydrogen was set equal to 0.040. Hartree–Fock (HF) and MP2 polarizabilities calculated with the Spackman basis possess errors less than 15% and 5%, respectively. Therefore, we have chosen the 6-31G(+sd,+sp) basis to describe chloro- and fluorobenzene in their argon complexes. The total basis used for the halobenzene–argon complexes may be denoted as [7s4p2d1f/4s3p1d/3s1p].

For moderately sized basis sets such as the augmented DZ basis sets used in this work, BSSE corrections determined with the counterpoise procedure (CP) of Boys and Bernardi[27] are absolutely necessary within supermolecular perturbation theory.[28] In the case of aromatic Ar complexes, BSSEs can lead to changes in the interaction energy up to 100% and equally serious changes in the complex geometries. Therefore, we applied the CP method of Boys and Bernardi by employing dimer-centered basis sets (DCBS) for the monomers in all calculations. The investigation of the van der Waals complexes followed procedures (1)–(5).

(1) The geometries of chloro- and fluorobenzene were calculated at the MP2 level with the G3MP2large basis set of Curtiss and co-workers as recently described in connection with the G3 method.[29] G3MP2large corresponds to a 6-311++G(2df,2p) basis set for the first row atoms (including also H) and to a [6s4p3d2f] basis with contraction pattern [631111;4211;111;11] for second row atoms. At optimized geometries, one-electron properties and the static electric (dipole) polarizability tensor were calculated as MP2 response properties using the Spackman basis set.

(2) Keeping the geometry obtained in (1) frozen, the complex binding energy of Ar·C_6H_5–X was determined for a given location of the Ar atom above the ring that complied with the C_s-symmetry of the complex. For this purpose, the energies of Ar and C_6H_5–X were calculated in the DCBS.

(3) According to (2), a grid of energy points corresponding to different Ar positions in the vicinity of its equilibrium position was obtained and the corresponding complex binding energies ΔE(complex) fitted to a polynomial depending on the parameters $R_\perp$ and $R_\parallel$ of Ar (Fig. 2).

(4) The equilibrium position of Ar corresponding to a maximal complex binding energy ΔE(complex) was determined and the properties of the Ar complex were calculated for its equilibrium geometry.

(5) Difference electron density distributions $\Delta\rho(\mathbf{r})$

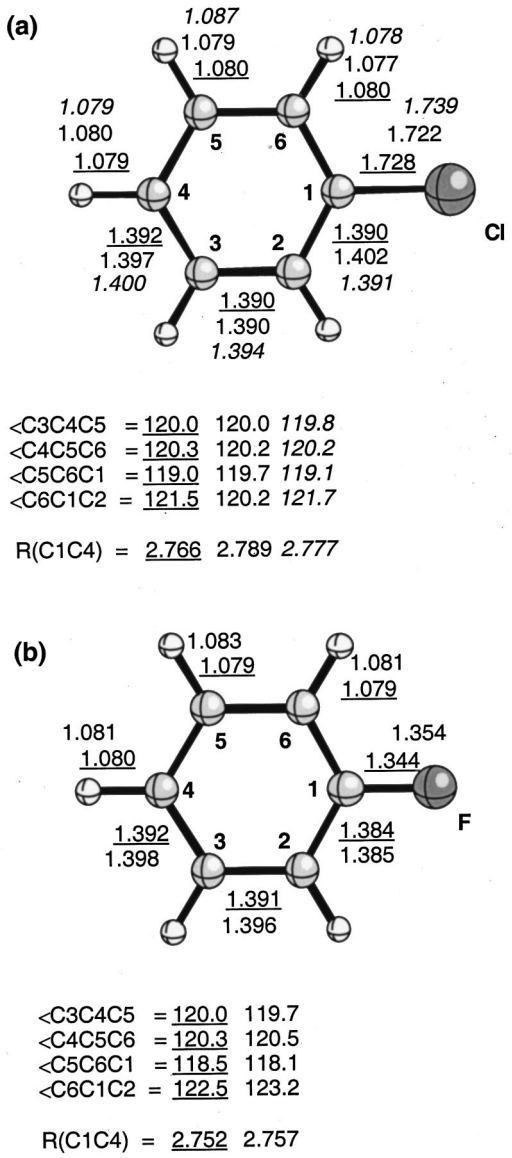

FIG. 3. Geometries of (a) chlorobenzene and (b) fluorobenzene calculated with the G3MP2large basis of Curtiss and co-workers (underlined values). Experimental values for chlorobenzene and fluorobenzene are from Ref. 33 (Cl: 33a: normal font; 33b: italics) and Ref. 34 (F). Distances in Å, angles in deg.

$=\rho(\text{complex})-\rho(\text{Ar,DCBS})-\rho(\text{benzene–X,DCBS})$ were determined for configuration **r** defining either the experimental or the calculated geometry of the complex.

Procedures (1)–(5) was applied to describe both chlorobenzene–argon and fluorobenzene–argon. All calculations were carried out using the COLOGNE2000 (Ref. 30) and ACESII (Ref. 31) *ab initio* packages.

In Table VI, calculated properties of chloro- and fluorobenzene as well as of the corresponding Ar complexes are summarized and, where possible, compared with the corresponding experimental data (for calculated geometries, see Fig. 3). The calculated dipole moments of chlorobenzene and fluorobenzene deviate from the corresponding experimental values by just -0.04 and -0.01 D [1.65 vs 1.69 (Ref. 32a) and 1.59 vs 1.60 D (Ref. 4), Table VI], respectively, while the isotropic polarizabilities differ by -0.3 [chlorobenzene, 12.0 vs 12.3 Å^3 (Ref. 36)] and -0.4 Å^3 [fluorobenzene, 9.9 vs 10.3 Å^3 (Ref. 36)]. Hence, agreement between theory and experiment is satisfactory and, in particular, both halogenobenzenes are described by theory with comparable accuracy, which is the basis for the following discussion.

Dipole moment μ and quadrupole moment Q of the Cl derivative are somewhat larger than the corresponding quantities of the F derivative[32] where for the complex formation in particular the difference in the Q_{cc} components matters. The differences in μ and Q are simply a result of the fact that the C–Cl bond is longer [1.728 Å; expt., 1.722 Å (Ref. 33)] than the C–F bond [1.344 Å; expt., 1.354 Å (Ref. 34)] and, by this, partial charges are separated over a larger distance in chlorobenzene than in fluorobenzene. Actually, the absolute magnitude of partial charges is larger in the latter molecule than in the former as is reflected by calculated natural atomic charges. Because of the large electronegativity of F, there is a strong withdrawal of σ-charge from the adjoined C atom in the benzene ring, which is slightly reduced by π-backdonation from the F atom to the benzene ring. Since σ-withdrawal dominates, the ipso C atom is strongly positively charged, which in turn leads to a shortening of the bonds $C_{ipso}-C_{ortho}$, and to a slightly smaller benzene ring as reflected by the distance C1–C4 (Fig. 3).

Actually the overall electronic effects of a Cl or a F atom on the benzene ring are somewhat larger for the latter as is indicated by the MP2/G3MP2large reaction energies [experimental reaction enthalpies derived from heat of formation $\Delta H_f^0(298)$] of isodesmic reactions such as (1) (7.0 and 7.9 kcal/mol, Table VI; experimental values[35–37] are 4.9 and 12.5 kcal/mol) or (2) (1.1 and 0 kcal/mol; experimental values[35–37] are 3.7 and 7.1 kcal/mol),

$$C_6H_5–X+CH_4\rightarrow C_6H_6+CH_3–X, \tag{1}$$

$$C_6H_5–X+CH_2{=}CH_2\rightarrow C_6H_6+CH_2{=}CHX. \tag{2}$$

Therefore, it is difficult to predict properties of the Ar complexes by just considering differences in the electron density distributions of the benzene rings of the two halobenzenes. A better basis for predicting complex properties is provided by comparing MP2 polarizabilities of the halobenzenes.

The isotropic dipole polarizability of chlorobenzene is 12.0 Å^3, which is clearly larger than that of fluorobenzene (9.9 Å, Table VI) where the difference results in particular from the a components, but there is also a difference of 1.2 Å^3 in the $c(\pi)$ components, which is relevant for the complex formation (Table VI). From the data of Table VI, we can predict that both dispersion forces and induced forces are larger in the case of the chlorobenzene–argon complex and that this should be reflected in a somewhat shorter distance $R_\perp$ and a somewhat larger complexation energy as compared to the corresponding parameters of the fluorobenzene–argon complex.

These predictions are in line with the calculated properties of the two complexes (Table VI). Both distance $R_\perp$ (Cl, 3.560; F, 3.588 Å) and $R_\parallel$ (Cl, 0.233; F, 0.154 Å) reflect the somewhat larger stability of the chlorobenzene complex (1.28 vs 1.17 kcal/mol, Table VI). The calculated Ar position for the chlorobenzene dimer compares reasonably with the

experimental position (3.56 vs 3.54 Å; 0.233 vs 0.387, Table VI) where the largest discrepancy is found for the lateral shift towards the substituted C1 atom (Fig. 2). Hence calculations confirm structure I as the correct structure for chlorobenzene–argon, the closer approach of the Ar atom toward the ring, and the stronger shift of Ar toward C–Cl relative to the corresponding values calculated for the fluorobenzene–argon complex.

V. DISCUSSION

In Fig. 4(a), a contour line diagram of the MP2 difference electron density distribution $\Delta\rho(\mathbf{r})$ of the chlorobenzene–Ar complex (BSSE corrected) is shown with regard to a plane containing the Ar atom, the center of the benzene ring, the C4–H bond, and the C1–Cl bond. There is a regular pattern of regions with increase (solid contour lines) and decrease (dashed contour lines) of electron density because of complex formation. Electron density is pushed out of the intermolecular region [region 3 in Fig. 4(a)] toward the back of the Ar atom (region 1) and through the center of the benzene ring (regions 4 and 10). If a nucleus stops this movement of negative charge, a build up of electron density can be found in front of the nucleus [region 2 in front of the Ar, regions 5a, 5b, and 6 in front of the C atoms and Cl, Fig. 4(a)]. Overall, regions of positive $\Delta\rho(\mathbf{r})$ are followed by regions of negative $\Delta\rho(\mathbf{r})$ in a regular pattern.

We note that there is just a small charge transfer of 1.5 melectron from the Ar atom toward the ring (donation into the π^* MOs of the phenyl ring in the sense of a donor–acceptor complex) even though the pattern of negative and positive difference densities might suggest a larger charge transfer. The magnitude of the charge transfer can only correctly be obtained if atomic charges are BSSE corrected (relatively large charge transfer values are obtained before BSSE corrections in particular by the Mulliken population analysis). However, if this is done both the natural bond orbital (NBO) and the Mulliken analysis lead to the same result for the fluoro- (1.5 melectron) and chlorobenzene complex (1.6 melectron).

The observed pattern in the $\Delta\rho(\mathbf{r})$ distribution of the chlorobenzene–argon complex is a result of exchange repulsion and mutual charge polarization between the complex partners. The optimal position of the Ar atom is above the benzene ring because in this region destabilizing exchange repulsion effects are minimal while at the same time the Ar atom can interact with all C atoms via stabilizing dispersion and induction interactions. If the charge distribution of the benzene ring is extended by a substituent such as Cl, the Ar atom can increase stabilizing dispersion interactions by moving towards the substituted C atom and interacting in this way with 7 rather than just 6 heavy atoms in a similar way. The C–X bond length and the polarizability of the X atom influence the value of the shift parameter $R_{\|}$: A larger C–X bond length (X polarizability) leads to a larger $R_{\|}$ value as found when comparing the chlorobenzene and fluorobenzene complex.

The pattern of regions with positive and negative difference densities found for the chloro- and fluorobenzene–Ar complex closely resembles that previously obtained for the benzene–Ar complex.[11] However, there are also some differences resulting from the presence of a halogen substituent. It seems as if in the complex the effective electronegativity of the C atoms is slightly increased (relative to the monomer

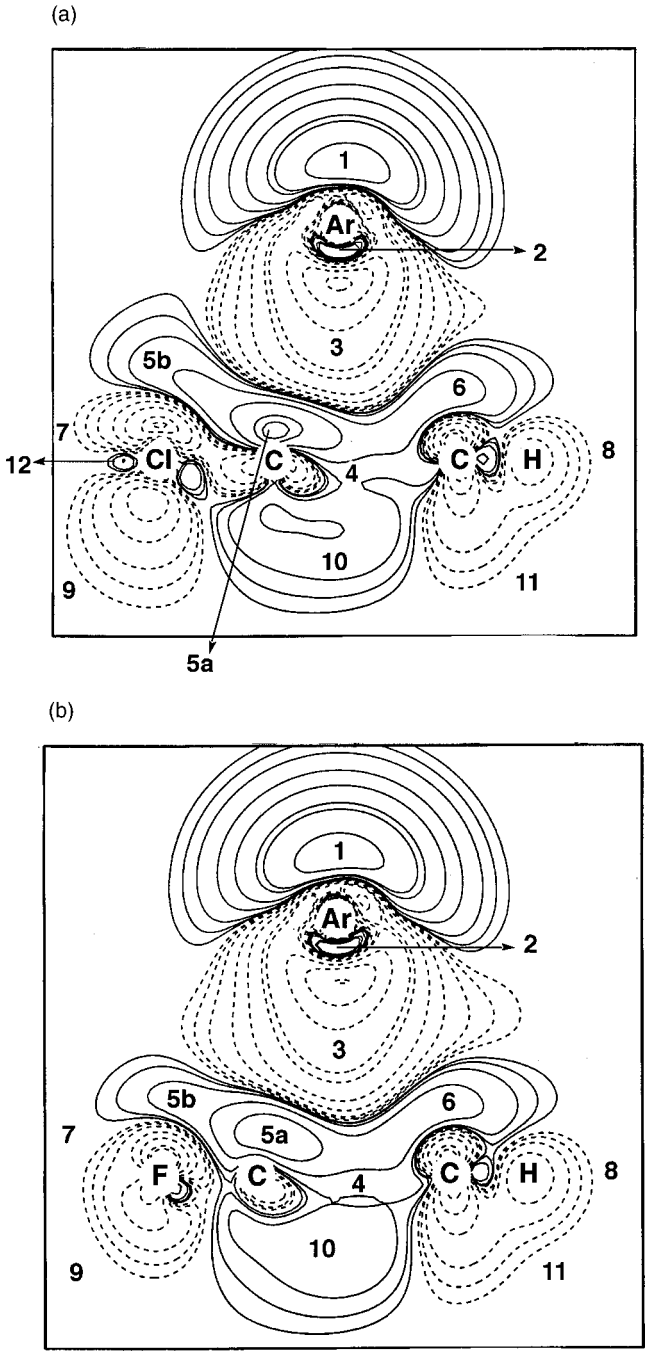

FIG. 4. Contour line diagram of the MP2 difference electron density distribution of (a) chlorobenzene–argon and (b) fluorobenzene–argon calculated with a $[7s4p2d1f/4s3p1d/3s1p]$ basis at optimized geometries. Reference plane is the plane perpendicular to the benzene ring that contains Ar and the C1–X/C4–H bonds. Contour lines range from 2×10^{-6} to about $2\times10^{-3}(e/\mathrm{Bohr}^3)$. For example, the contour levels in region 1 are (from outermost to innermost level): 0.2, 0.3, 0.7, 2, 3, 7, 8, 20 in units of $10^{-5}\ e/\mathrm{Bohr}^3$ ($1\ e/\mathrm{Bohr}^3 = 6.748\,315\ e/\text{Å}^3$). Outermost levels in regions 3, $4+5+6+10$: $0.2\times10^{-5}\ e/\mathrm{Bohr}^3$. Solid lines correspond to an increase of electron density upon complex formation, dashed lines to a decrease. Regions of increase and decrease of electron density are marked by small numbers.

situation) thus leading to a slight charge transfer from H and X atoms toward the C atoms where for X this charge transfer takes place predominantly in the π-space. Two effects could be responsible for these changes. (a) The Ar atom pushes density (via exchange repulsion) through the center of the ring, which also leads to a loss of σ-density of the C atoms, an increase of the effective nuclear charge of the C atoms and the possibility of contracting the π-density stronger, i.e., the effective electronegativity of the C atoms increases in the π-space. (b) The larger size of the Cl atom and by this the larger exchange repulsion between Cl and Ar is visible by a built-up of positive difference density in the outer valence region of Cl [region 5(b), Fig. 4(a)]. It hinders the Ar atom from moving further into the C–Cl direction, but it leads also to pushing π-density out of the inner valence region back to the C atom, which has a smaller size and by this also smaller exchange repulsion. Hence, C can take some small amount of π-charge from the Cl atom balancing this by backdonation in the σ-space (region 12). The small loss of electron density at the Cl atom is confirmed by a slight reduction of the dipole moment in the chlorobenzene–argon complex (see μ_a, Table VI).

Since the difference density distribution of the fluorobenzene–argon complex [Fig. 4(b)] is similar to that of the corresponding chlorobenzene complex [Fig. 4(a)], we have made differences between the density distributions of the two complexes visible by recalculating the fluorobenzene complex in the geometry of the chlorobenzene complex (keeping the CF bond length). In this way, it is possible to derive a difference density distribution,

$$\Delta\Delta\rho(\mathbf{r}) = [\rho(\mathrm{Cl-complex}) - \rho(\mathrm{Ar,DCBS}) - \rho(\mathrm{benzene-Cl,DCBS})] - [\rho(\mathrm{F-complex}) - \rho(\mathrm{Ar,DCBS}) - \rho(\mathrm{benzene-F,DCBS})],$$

which apart from the region close to the C–X bond can be considered to represent differences caused by the replacement of Cl by F. The contour line diagram in Fig. 5 verifies the larger size of the Cl atom, which leads to a polarization of the electron density at the Ar atom; density is pushed from the Cl side of the Ar atom (region 1) to the opposite side (region 2). Hence, the asymmetry in the difference density in regions 5 and 6 of Fig. 4 has its equivalent in region 1 as made visible in Fig. 5. It reflects the larger polarizing ability of the Cl atom (more electrons, larger size, stronger exchange repulsion) as opposed to that of the F atom.

Table V lists structural parameters for several halogenated aromatic–Ar complexes which have been analyzed with the Bauder model,[20] in so far as possible, for consistency. As discussed more fully recently,[5] small differences of about 0.01–0.02 Å between the parameters are likely meaningful indicators of actual trends in equilibrium parameters. $R_\perp$, the perpendicular distance of the argon from the ring, is a useful indicator of trends in van der Waals complexes since it should be related to electronic effects and presumably with interaction strength. One observes the aforementioned trend of closer approach to the ring with increased fluorination. What is also striking is that the argon is closer to the ring in chlorobenzene compared to benzene, fluorobenzene, and even difluorobenzenes.

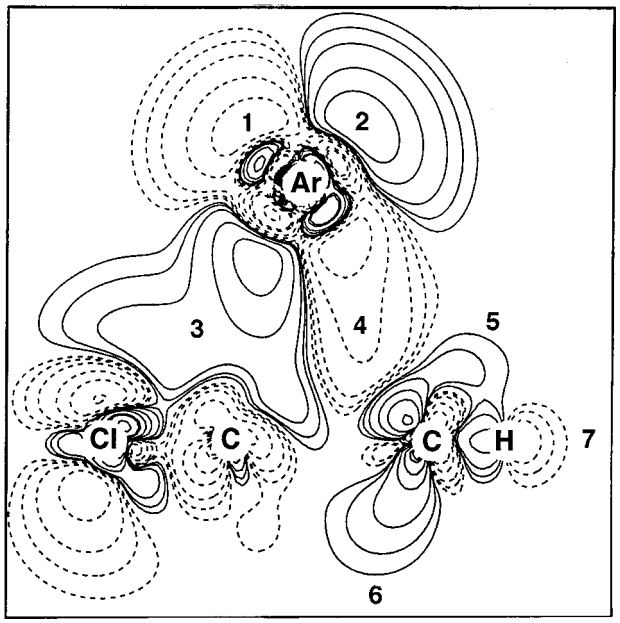

FIG. 5. Contour line diagram of the MP2 difference difference electron density distribution $\Delta\Delta\rho(\mathbf{r}) = \Delta\rho(\text{chlorobenzene–Ar}) - \Delta\rho(\text{fluorobenzene–Ar})$ using the $[7s4p2d1f/4s3p1d/3s1p]$ basis set. Fluorobenzene–argon is kept (apart from the F atom) at the geometry of the chlorobenzene–argon complex to guarantee a meaningful $\Delta\Delta\rho(\mathbf{r})$. Reference plane is the plane perpendicular to the benzene ring that contains Ar and the C1–X/C4–H bonds. Contour lines range from 2×10^{-6} to about 2×10^{-3} e/Bohr^3. For example, the contour levels in region 1+4 are (from outermost to innermost level): −0.2, −0.3, −0.7, −2, −3 in units 10^{-5} e/Bohr^3 (1 e/Bohr^3 = 6.748 315 e/Å^3). Outermost levels in regions 2 and 3: 0.2×10^{-5} e/Bohr^3. Solid lines correspond to an increase of electron density upon complex formation, dashed lines to a decrease.

These trends are easily explained by considering what has been learned from the chlorobenzene–fluorobenzene comparison. Induction forces between Ar and an aromatic ring are small as was recently observed in the case of the oxazole–argon[11] or isoxazole–argon[12] complexes and as is confirmed in the present case (dipole moment component in *c*-direction, 0.05 D, Table VI). Hence, the stability and geometry of an Ar complex are determined by an energetic balance based on the maximization of dispersion interactions in connection with a minimization of exchange repulsion interactions. Stepwise replacement of H atoms by the more polarizable F atoms leads to a stepwise increase of stabilizing dispersion interactions provided the Ar can move in the direction of the substituent(s). This is measured by the parameter $R_\parallel$ which is zero for benzene–Ar and increases with the size of the substituent X and the number of substituents in an asymmetrical substitution pattern (see Table V).

One can deduce from these factors that for increasing size of X, Ar must come closer to the substituted C atom (larger $R_\parallel$; distance Ar–carbon1 decreases: 3.85 Å for benzene–Ar, 3.75 Å for fluorobenzene–Ar; 3.68 Å for chlorobenzene–Ar). This is parallel to a decrease of $R_\perp$ (3.586; 3.572; 3.540 Å) and an increase in the complex binding energy (1.12; 1.17; 1.28 kcal/mol). This conclusion agrees with previous multiphoton ionization spectra.[13,14,38]

We conclude that the properties of van der Waals complexes between Ar and aromatic compounds can be easily understood considering the interplay of dispersion and exchange repulsion forces where these factors can be assessed considering (a) the topology of the aromatic compound, (b) the polarizability, and (c) the size (number of electrons) of the atoms forming the aromatic compound.

We note that the topology of the previously investigated benzene–, oxazole–, and isoxazole–argon complexes[11,12] is basically different from that of the substituted benzene–argon complexes discussed in this work. In the first case, the Ar atom stays above the ring center (benzene–argon) or moves closer to one of the heteroatoms in the ring provided exchange repulsion forces are smaller for this particular atom (contraction of the density in case of more electronegative atoms). Hence, the shift of the Ar atom is determined by the electronic properties of the atoms forming the ring. In the latter case, the shift direction of the Ar atom is influenced by the topology of the substitution pattern because the Ar atom wants to increase the number of stabilizing dispersion interactions with nonhydrogen atoms. Exchange repulsion plays a minor role, but determines the actual magnitude of distance $R_{\perp}$ and the shift parameter $R_{\parallel}$. We are presently investigating the question whether the interaction patterns discussed in the present work apply also to other noble gas van der Waals complexes.

ACKNOWLEDGMENTS

J.J.O. acknowledges support by the Ministry of Science and Technology in Korea (MOST) under 99-B-WB-07-A-03. This work was supported at Ann Arbor by the National Science Foundation, Washington, D.C. with a grant from the Experimental Physical Chemistry Division to the University of Michigan and at Göteborg University by the Swedish Natural Science Research Council (NFR). All quantum chemical calculations were done on the CRAY C90 of the Nationellt Superdatorcentrum (NSC), Linköping, Sweden. E.K. and D.C. thank the NSC for a generous allotment of computer time.

[1] A. Bauder, J. Mol. Struct. **408**, 33 (1997).
[2] For example, for the benzene–argon system see H. Koch, B. Fernández, and O. Christiansen, J. Chem. Phys. **108**, 2784 (1998), and references therein.
[3] Th. Brupbacher, J. Makarewicz, and A. Bauder, J. Chem. Phys. **101**, 9736 (1994).
[4] R. A. Appleman, S. A. Peebles, and R. L. Kuczkowski, J. Mol. Struct. **446**, 55 (1998).
[5] R. J. Wilson, S. A. Peebles, S. Antolínez, M. E. Sanz, and R. L. Kuczkowski, J. Phys. Chem. A **102**, 10630 (1998).
[6] R. Sussmann, R. Neuhauser, and H. Neusser, Can. J. Phys. **72**, 1179 (1994).
[7] R. M. Spycher, L. Hausherr-Primo, G. Grassi, and A. Bauder, J. Mol. Struct. **351**, 7 (1995).
[8] M. Onda, H. Mukaida, H. Akiba, M. Mori, H. Miyazaki, and I. Yamaguchi, J. Mol. Spectrosc. **169**, 480 (1995).
[9] M. Onda, Y. Bitoh, and A. R. Hight Walker, J. Mol. Struct. **410**, 51 (1997).
[10] E. Jochims, H. Mäder, and W. Stahl, J. Mol. Spectrosc. **180**, 116 (1996).
[11] E. Kraka, D. Cremer, U. Spoerel, I. Merke, W. Stahl, and H. Dreizler, J. Phys. Chem. **99**, 12466 (1995).
[12] U. Spoerel, H. Dreizler, W. Stahl, E. Kraka, and D. Cremer, J. Phys. Chem. **100**, 14298 (1996).
[13] M. Mons, J. Le Calvé, F. Piuzzi, and I. Dimicoli, J. Chem. Phys. **92**, 2155 (1990).
[14] M. Mons and J. Le Calvé, Chem. Phys. **146**, 195 (1990).
[15] T. J. Balle and W. H. Flygare, Rev. Sci. Instrum. **52**, 33 (1981).
[16] J.-U. Grabow, Ph.D. thesis, University of Kiel, 1992.
[17] H. M. Pickett, J. Mol. Spectrosc. **148**, 371 (1991).
[18] J. K. G. Watson, J. Chem. Phys. **46**, 1935 (1967).
[19] T. D. Klots, T. Emilsson, R. S. Ruoff, and H. S. Gutowsky, J. Phys. Chem. **93**, 1255 (1989).
[20] R. M. Spycher, D. Petitprez, F. L. Bettens, and A. Bauder, J. Phys. Chem. **98**, 11863 (1994).
[21] Z. Kisiel, J. Mol. Spectrosc. **144**, 381 (1990).
[22] R. L. Poynter, J. Chem. Phys. **39**, 1962 (1963).
[23] (a) C. Møller and M. S. Plesset, Phys. Rev. **46**, 618 (1934); (b) For a recent review see, D. Cremer, in *Encyclopedia of Computational Chemistry*, edited by P. v. R. Schleyer, N. L. Allinger, T. Clark, J. Gasteiger, P. A. Kollman, H. F. Schaefer III, and P. R. Schreiner (Wiley, Chichester, 1998), Vol. 3, p. 1706.
[24] G. Chałasínski, D. J. Funk, J. Simons, and W. H. Breckenridge, J. Chem. Phys. **87**, 3569 (1987).
[25] M. A. Spackman, J. Phys. Chem. **93**, 7594 (1989).
[26] P. C. Hariharan and J. A. Pople, Chem. Phys. Lett. **16**, 217 (1972).
[27] S. F. Boys and F. Bernardi, Mol. Phys. **19**, 553 (1970).
[28] For a review on the basis set superposition problem, see F. B. van Duijneveldt, J. G. C. M. van Duijneveldt-van de Rijdt, and J. H. van Lenthe, Chem. Rev. **94**, 1873 (1994).
[29] L. A. Curtiss, P. C. Redfern, K. Raghavachari, V. Rassolov, and J. A. Pople, J. Chem. Phys. **110**, 4703 (1999).
[30] E. Kraka, J. Gräfenstein, J. Gauss, F. Reichel, L. Olsson, Z. Konkoli, Z. He, Y. He, and D. Cremer, COLOGNE2000 (Göteborg University, Göteborg, 2000).
[31] (a) J. F. Stanton, J. Gauss, J. D. Watts, W. J. Lauderdale, and R. J. Bartlett, ACES II, Quantum Theory Project, University of Florida, 1992; (b) See also J. F. Stanton, J. Gauss, J. D. Watts, W. J. Lauderdale, and R. J. Bartlett, Int. J. Quantum Chem., Symp. **26**, 879 (1992).
[32] For dipole moments and quadrupole moments of chlorobenzene and fluorobenzene, see (a) R. D. Nelson, Jr., D. R. Lide, Jr., and A. A. Maryott, Natl. Stand. Ref. Data Ser. (U.S., Natl. Bur. Stand.) **10** (1967); (b) J. Hernandez-Trujillo and A. Vela, J. Phys. Chem. **100**, 6524 (1996).
[33] (a) M. Onda, Nippon Kagaku Kaishi **11**, 1476 (1986); (b) S. Cradock, J. M. Muir, and D. W. H. Rankin, J. Mol. Struct. **220**, 205 (1990).
[34] S. Doraiswamy and S. D. Sharma, J. Mol. Struct. **102**, 81 (1983).
[35] M. R. Zachariah, P. R. Westmoreland, D. R. Burgess, Jr., W. Tsang, and C. F. Melius, J. Phys. Chem. **100**, 8737 (1996).
[36] J. D. Cox and G. Pilcher, *Thermochemistry of Organic and Organometallic Compounds* (Academic, London, 1970).
[37] J. B. Pedley, R. D. Naylor, and S. P. Kirby, *Thermochemical Data of Organic Compounds*, 2nd ed. (Chapman and Hall, New York, 1986).
[38] E. J. Bieske, M. W. Rainbird, J. M. Atkinson, and A. E. W. Knight, J. Chem. Phys. **91**, 752 (1989).
[39] *CRC Handbook of Chemistry and Physics on CD-ROM, 2000 Version*, edited by D. R. Lide (CRC, Cleveland, 2000).